

A numerical ocean circulation model of the Norwegian and Greenland Seas

DAVID P. STEVENS

School of Mathematics, University of East Anglia, Norwich NR4 7TJ, UK

Abstract – The dynamics and thermodynamics of the Norwegian and Greenland Seas are investigated using a three-dimensional primitive equation ocean circulation model. The horizontal resolution of the model is 1° in the zonal direction and 0.5° in the meridional direction. The vertical structure is described by 15 levels. The model is driven by both annual mean and seasonally varying wind and thermohaline forcing. The connections of the Norwegian and Greenland Seas with the North Atlantic and Arctic Ocean are modelled with an open boundary condition. The simulated currents are in reasonable agreement with the observed circulation.

CONTENTS

1.	Introduction	365
2.	The Numerical Model	368
3.	The Model Domain, Grid and Parameters	370
4.	Annual Mean Forcing	371
5.	A Seasonal Study	379
	5.1 Initial and boundary data	379
	5.2 Integrated quantities	382
	5.3 Horizontal sections	386
	5.4 Vertical sections	393
6.	Conclusion and Future Improvements	400
7.	Acknowledgements	401
8.	References	401

1. INTRODUCTION

The Norwegian and Greenland Seas situated between Norway and Greenland are bounded to the south by the Greenland Scotland ridge and to the north by Spitsbergen (Svalbard) and the Fram strait. There are two main basins in the region, the Norwegian basin in the south and the Greenland basin to the north. There are many interesting and complex oceanographic phenomena taking place in the region. Warm saline water flows into the region from the North Atlantic between the Shetland Isles and the Faroes. As this water is advected north it is cooled and becomes more dense. The Greenland Sea is an area of intense cooling where the surface waters are cooled so much that the water column becomes unstable and overturns forming bottom water. Various authors have speculated on how bottom water is formed. CARMACK and AAGAARD (1973) propose a sub-surface modification of the North Atlantic water in the Greenland gyre based on a double diffusive process. KILLWORTH (1979) suggests formation by "chimneys", narrow

interest and have little effect on the flow there. SEMTNER (1987) extended his 1976 model by including more realistic surface forcing and a sea ice model. The predicted currents in the above three models are rather low. This is because of the excessively large eddy viscosities used for computational stability. Finally, the work of LEGUTKE (1986) must be noted, although only a limited amount has yet been published. She uses a similar approach to that used here although the horizontal resolution is higher and the domain of interest is slightly smaller. [Ed: see this issue.]

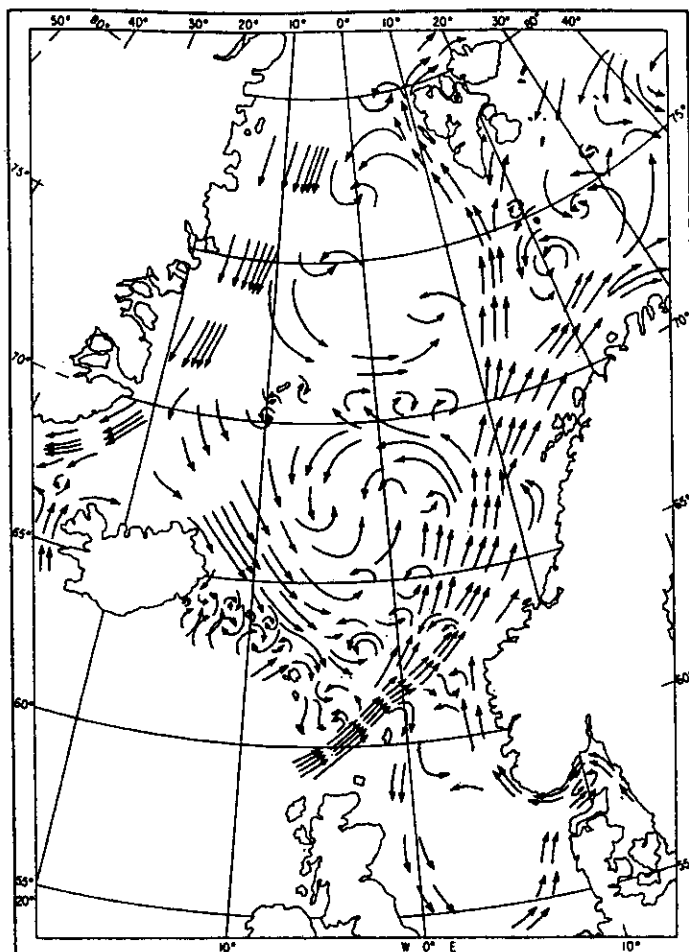


FIG.1. Schematic of the surface circulation taken from METCALF (1960).

The equations of motion are rearranged to form an equation for the barotropic stream function ψ :

$$\begin{aligned} & \left[\frac{\partial}{\partial \lambda} \left(\frac{1}{H \cos \phi} \frac{\partial^2 \psi}{\partial \lambda \partial t} \right) + \frac{\partial}{\partial \phi} \left(\frac{\cos \phi}{H} \frac{\partial^2 \psi}{\partial \phi \partial t} \right) \right] - \left[\frac{\partial}{\partial \lambda} \left(\frac{f}{H} \frac{\partial \psi}{\partial \phi} \right) - \frac{\partial}{\partial \phi} \left(\frac{f}{H} \frac{\partial \psi}{\partial \lambda} \right) \right] \\ & = - \left[\frac{\partial}{\partial \lambda} \left(\frac{g}{\rho_0 H} \int_{-H}^0 \int_z^0 \frac{\partial \rho}{\partial \phi} dz' dz \right) - \frac{\partial}{\partial \phi} \left(\frac{g}{\rho_0 H} \int_{-H}^0 \int_z^0 \frac{\partial \rho}{\partial \lambda} dz' dz \right) \right] \\ & + \left[\frac{\partial}{\partial \lambda} \left(\frac{a}{H} \int_{-H}^0 F^v - \Gamma(v) dz \right) - \frac{\partial}{\partial \phi} \left(\frac{a \cos \phi}{H} \int_{-H}^0 F^u - \Gamma(u) dz \right) \right] \end{aligned} \quad (7)$$

where

$$-\frac{1}{a} \frac{\partial \psi}{\partial \phi} = \int_{-H}^0 u dz, \quad \frac{1}{a \cos \phi} \frac{\partial \psi}{\partial \lambda} = \int_{-H}^0 v dz$$

and F^u , F^v are the diffusive terms on the right hand side of equations (1), (2) respectively.

Details of the equations for the baroclinic velocities and the method of solution have been given by various authors (BRYAN, 1969; SEMTNER, 1974; COX, 1984; and SEMTNER, 1986). The finite difference grid used is that of the Arakawa "B" type, in which tracer points T and stream function points ψ are placed in the centre of cells and the horizontal velocity components u , v are situated at the corners. In the vertical T , u , v are located in the centre of the cell. Time stepping is achieved by leapfrogging, with the associated time splitting removed by a Robert time filter as described by ASSELIN (1972).

At the surface the model is driven by a prescribed wind stress and buoyancy forcing. The usual no slip and no flux of tracer conditions are applied at lateral boundaries. A no flux of tracer condition is specified at the ocean floor. A further condition at the ocean floor is that of bottom friction, which is applied through a square law with a drag coefficient of 1.3×10^{-3} and a 10° turning angle resulting from Ekman effects. Further details of the boundary conditions applicable at natural land boundaries have been given in the above four articles.

The boundary condition at open ocean boundaries is based on that of STEVENS (1990). This method calculates variables at the boundary from dominant terms in the governing equations. The baroclinic velocity field is determined from the momentum equations (1) and (2) with two modifications. Firstly the nonlinear terms which are small throughout much of the ocean are neglected. Secondly the unknown value in the diffusion term (which lies outside the model domain) is approximated by the value on the boundary. The treatment of tracers depends upon whether there is inflow or outflow at a point on the boundary at a given time. At inflow points information propagates inwards from a region which is not modelled, so tracers are relaxed to observed values. At points where there is either advection or wave propagation outwards, tracers are calculated from terms involving that advection or wave propagation normal to the boundary and a diffusion term which is modified in a similar way to that in the momentum equations. The calculation of the stream function at open boundaries provides the greatest difficulty. There are no tractable simplifications to the equation (7) describing the stream function ψ that are generally applicable. The choice of boundary condition for the stream function is discussed in section 4.

of the horizontal grid is reduced from 76 by 51 points to 54 by 51 points, this increases computational efficiency and reduces storage requirements.

Vertical mixing in the ocean is still poorly understood and poorly treated in general circulation models. The vertical mixing coefficients K_m and K_h are not limited by any stability criteria for any realistic range of values. For this study a simplistic approach is taken. A constant value of $1\text{cm}^2\text{s}^{-1}$ is used for both K_m and K_h . There is no doubt that this value is rather large for the more stably stratified regions of the ocean and probably too small for the less stratified waters, but nevertheless it provides a compromise.

A realistic value for A_m is of the order of $10^6\text{cm}^2\text{s}^{-1}$. However, A_m has to be chosen large enough to eliminate computational noise (a common problem with large scale primitive equation models) and thus its value is dictated by the grid size. Details of stability criteria have been given by various authors, for instance BRYAN, MANABE and PACANOWSKI (1975) and KILLWORTH, SMITH and GILL (1984). The value of A_m used in this study is $10^8\text{cm}^2\text{s}^{-1}$. The stability criteria on the horizontal diffusivity A_h are not quite so severe, a more realistic value of $10^7\text{cm}^2\text{s}^{-1}$ is used.

Finally the length of timesteps needs to be decided. The convergence of the meridians to the north means that the diffusive condition is the most restrictive, namely

$$\Delta t < \frac{\Delta^2}{8A_m},$$

where Δt is the timestep and Δ is the width of the smallest grid box. This timestep limitation is well known and can be found in almost any text on numerical analysis, for example O'BRIEN (1986). Under the above condition a maximum timestep of 2900 seconds is allowed. However, for this study a timestep of 2700 seconds (45 minutes) is used.

4. ANNUAL MEAN FORCING

In this section annual mean surface forcing is used to drive the model ocean. The temperature and salinity fields throughout the model ocean are initialised using the LEVITUS (1982) climatology, whilst the velocity fields are started from rest. The initial density at the surface and the temperature and salinity fields at 520m are shown in Fig.3. Warm saline water of North Atlantic origin can be seen off the Norwegian coast. The fresh surface water at the coast is caused by fresh water runoff from rivers and fjords. To the west (off the Greenland coast) cold fresh East Greenland Current water of Arctic origin is apparent. The densest water occurs over the Greenland Sea basin. A further point of note is the smooth nature of the data.

The surface wind stress is obtained from 12 hourly NMC (National Meteorological Centre, USA) wind velocities for 1982, which are stored in 2.5° latitude longitude squares. The wind stress is calculated from the wind velocity using the following empirical formulae

$$\tau^{\lambda} = \rho_a c_d u_w |v_w|, \quad \tau^{\phi} = \rho_a c_d v_w |v_w|, \quad (8)$$

where ρ_a is the density of air, c_d is a drag coefficient and v_w is the wind velocity vector with components u_w and v_w . The relationship (8) has been used by many authors (for example GILL, 1982, p.29; SEMTNER, 1976b) with various formulae for the drag coefficient c_d , which is obtained by fitting experimental data. For this study the linear relationship of ANDERSON (personal communication)

$$c_d = 0.013(0.8 + 0.065|v_w|),$$

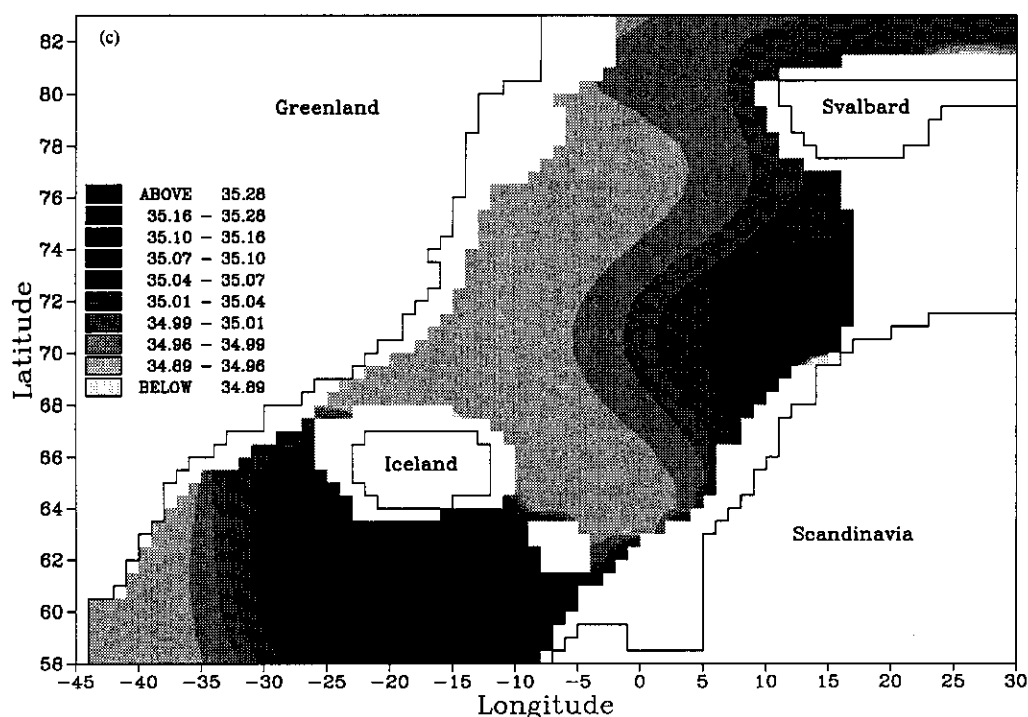


FIG.3. Annual mean (a) surface density ($\text{kg m}^{-3}\cdot 1000$), (b) temperature ($^{\circ}\text{C}$) at 520m, and (c) salinity (ppt) at 520m.

is used. The wind stresses are then averaged to produce an annual mean. Finally the wind stresses are interpolated from the 2.5° latitude, longitude grid onto the model grid using a bi-cubic spline interpolation procedure. Figure 4 shows the 1982 annual mean. The prominent cyclonic structure of the wind is clearly illustrated. South-westerlies blow northward past Scotland and Norway, whilst winds of polar origin blow southward adjacent to Greenland. This annual mean pattern is very representative of the wind, except for a few short spells in the spring and summer.

There is a choice of surface boundary conditions on tracers between prescribing values of temperature and salinity at the surface or specifying a flux. A flux condition is certainly the more pleasing condition to use, for in reality the ocean is driven by fluxes. It also allows the ocean surface waters far more freedom than prescribing tracers at the surface. However data for the region are sparse so the surface temperature and salinity are prescribed from annual mean LEVITUS (1982) data. The specification of surface values is used in the hope of making the model more realistic in the absence of reliable flux data. In fact prescribing tracer values on the surface level of such a model can almost be thought of as specifying a flux condition on the level below. Prescribing the surface value of salinity also has the advantage that the shallow coastal waters are continually kept fresh by the imposed data, thus retaining the effect of freshwater river runoff.

The final point to consider is the boundary data that needs to be fed into the open boundaries of the model. For the runs described in this article, the southern boundary is open between 45°W and 7°W , while the northern boundary is open between 4°W and 30°E . The only substantial sea

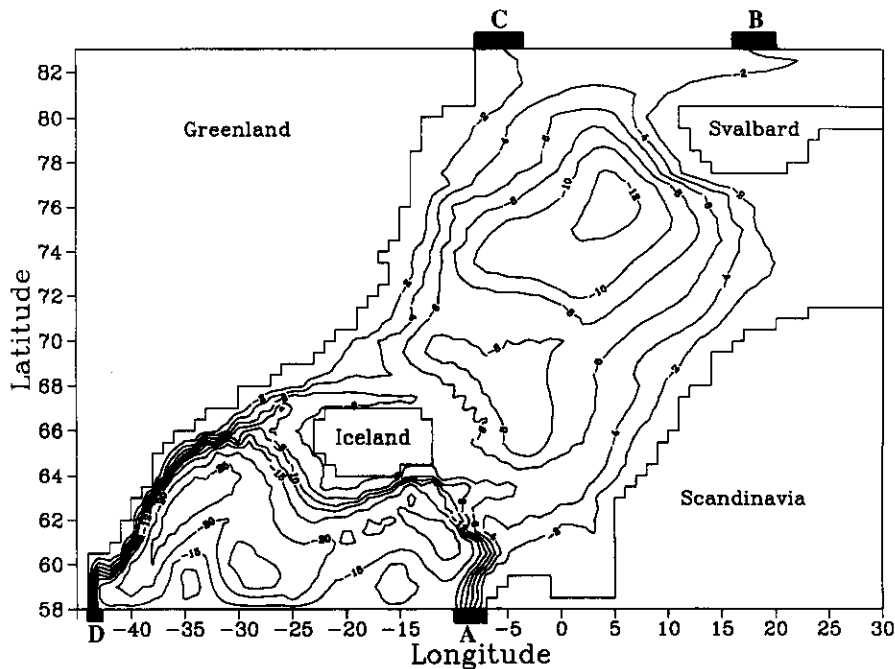


FIG.5. The stream function (in Sverdrups) after 1000 timesteps (31 days) using the estimates of WORTHINGTON (1970) for stream function boundary data. The contour interval is 2 Sverdrups between -2 and -12 Sverdrups and 5 Sverdrups for values less than -15 Sverdrups.

gap D in the south. While an exchange of 3 Sverdrups, outflow through gap B and inflow through gap C, took place with the Arctic Ocean. The large value of 13 Sverdrups inflow from the North Atlantic rather than the 8 Sverdrups suggested by Worthington is to compensate for the blocking effect of the Iceland-Scotland ridge. It was found that most of the water that was input through gap A would turn westwards, south of Iceland and head towards outflow D.

A run was performed using the boundary data described above. The resulting stream function field at 1000 timesteps (31 days) is shown in Fig.5. The inflow from the North Atlantic splits into two parts with one travelling northwards into the Norwegian Sea and the other heading westward to the south of Iceland. There is a region of cyclonic circulation over the Greenland Sea basin and a similar region of weaker circulation over the Norwegian Sea basin. With reference to Fig.2 it can be seen that the circulation is strongly controlled by topography. The circulation within the Norwegian and Greenland Seas looks reasonably realistic. However the same cannot be said of the region to the south of Iceland. There are a number of small strong gyres and a region of strong flow tangential to the southern boundary. Also large vertical velocities occur in the region close to the southern boundary. The main driving force of the barotropic flow in this region is the bottom pressure torque. It seems that this unphysical and undesirable behaviour of the stream function is brought about by the unsatisfactory boundary condition at the southern boundary. The boundary data are not consistent with the topography and the density field which forces the stream function. Thus the use of a few small regions for exchanges of water between ocean basins (and effectively what is a solid wall to the barotropic mode elsewhere) seems to be limited. This is especially so at the southern boundary where major exchanges of water masses take place. No such problems occur at the northern boundary where exchanges with the Arctic Ocean are on a much smaller scale. The stream function here is able to adjust within a single grid point from the

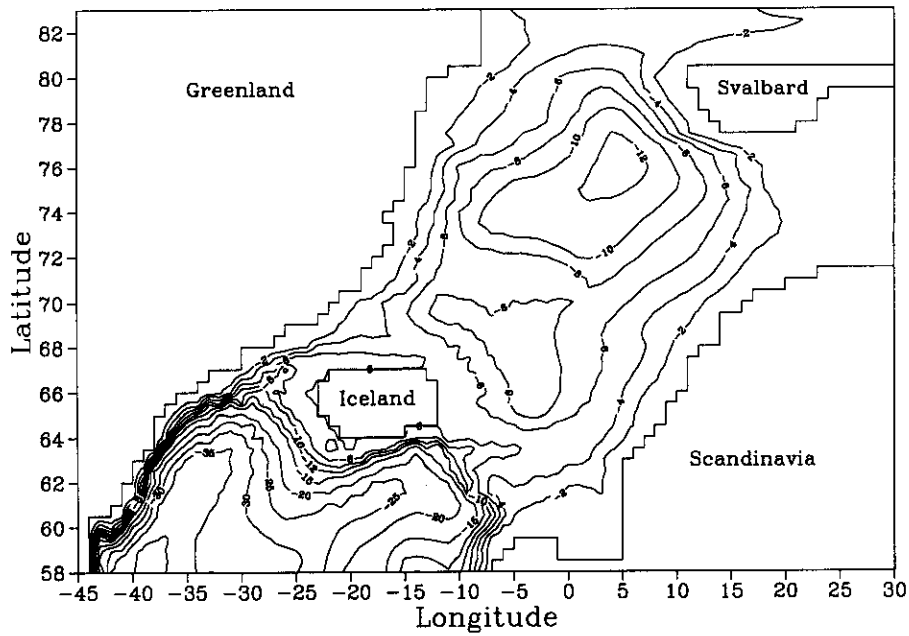


FIG.6. The stream function (in Sverdrups) after 1000 timesteps (31 days) forcing with mean surface data. The contour interval is 2 Sverdrups between -2 and -12 Sverdrups and 5 Sverdrups for values less than -15 Sverdrups.

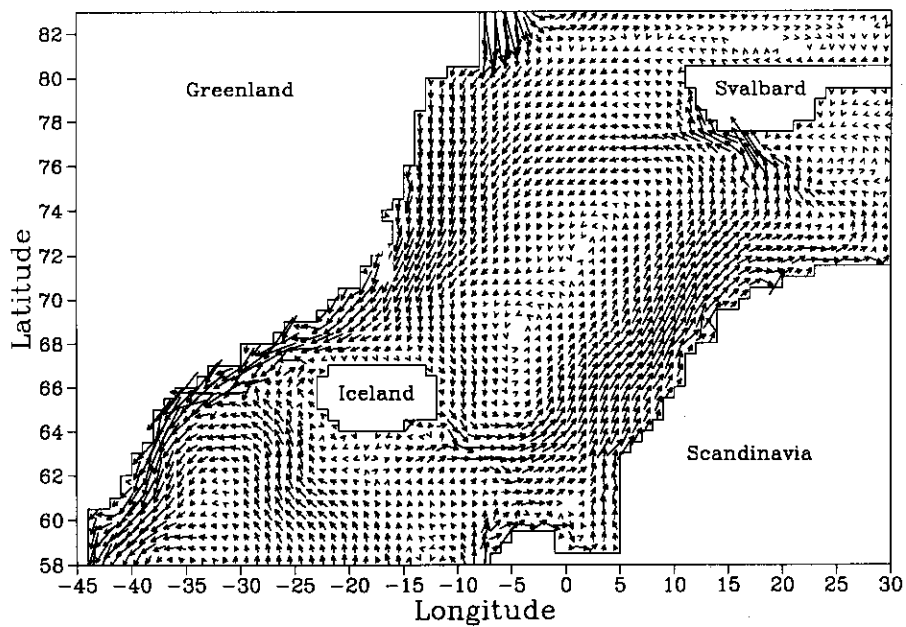


FIG.7. The velocity at level 2 (20m) after five years forcing with mean surface data. The distance between grid points corresponds to a speed of 5 cm s^{-1} .

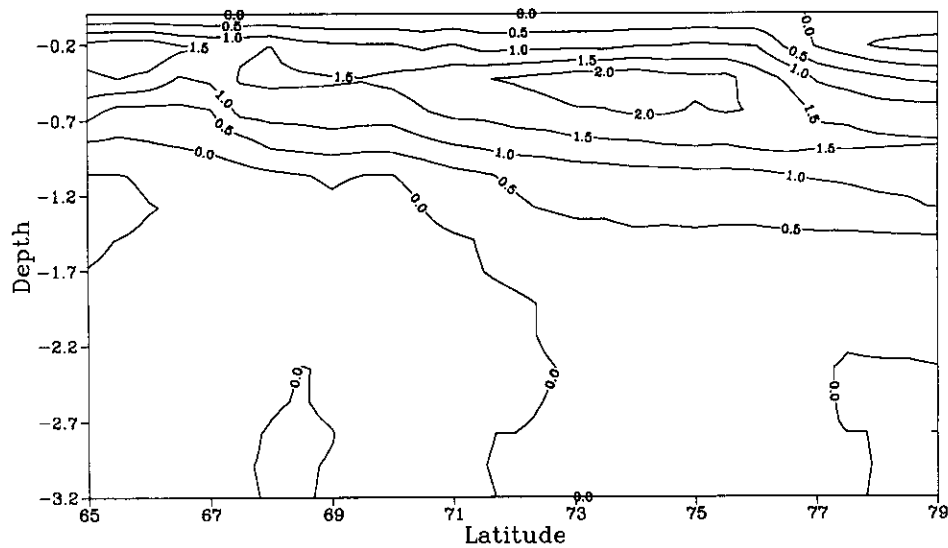


FIG.9. The zonally averaged meridional circulation (in Sverdrups) after five years forcing with mean surface data. The depth is in kilometres.

5. A SEASONAL STUDY

5.1 Initial and boundary data

The model described in the previous section has been employed to study the effect of seasonal forcing. The wind stresses used are monthly means derived (as described in section 4) from 12 hourly NMC winds for 1982 and 1983. Linear interpolation is used between each month to capture the seasonal variations while eliminating the high frequency variability that the use of 12 hourly winds produce. A further advantage is that it avoids the excessive computations involved in interpolating each 12 hourly wind onto the model grid. Most of the monthly mean winds are of a similar structure to the annual mean wind (see Fig.4). However there are a few exceptions such as April 1983 (Fig.10).

The thermohaline forcing is taken from an LEVITUS and OORT (1977). This was used because when the work was undertaken it was the only seasonal dataset easily available. Once more the temperature and salinity (and thus density) are prescribed at the sea surface. The surface density for the summer and winter seasons are shown in Fig. 11. Comparing these figures with Fig.3 it can be seen that the basic structure of the fields is quantitatively similar to that of the mean data. As would be expected the water is warmer in summer, especially the North Atlantic inflow water that is advected northwards along the Norwegian coast. Also the summer surface water is fresher, presumably as a result of melting sea ice and increased runoff of melt water from land. The winter water is more saline, as a lot of fresh water is locked up in snow and ice and thus is unavailable to freshen the Atlantic inflow to the same extent as in the summer. In the winter the water can be

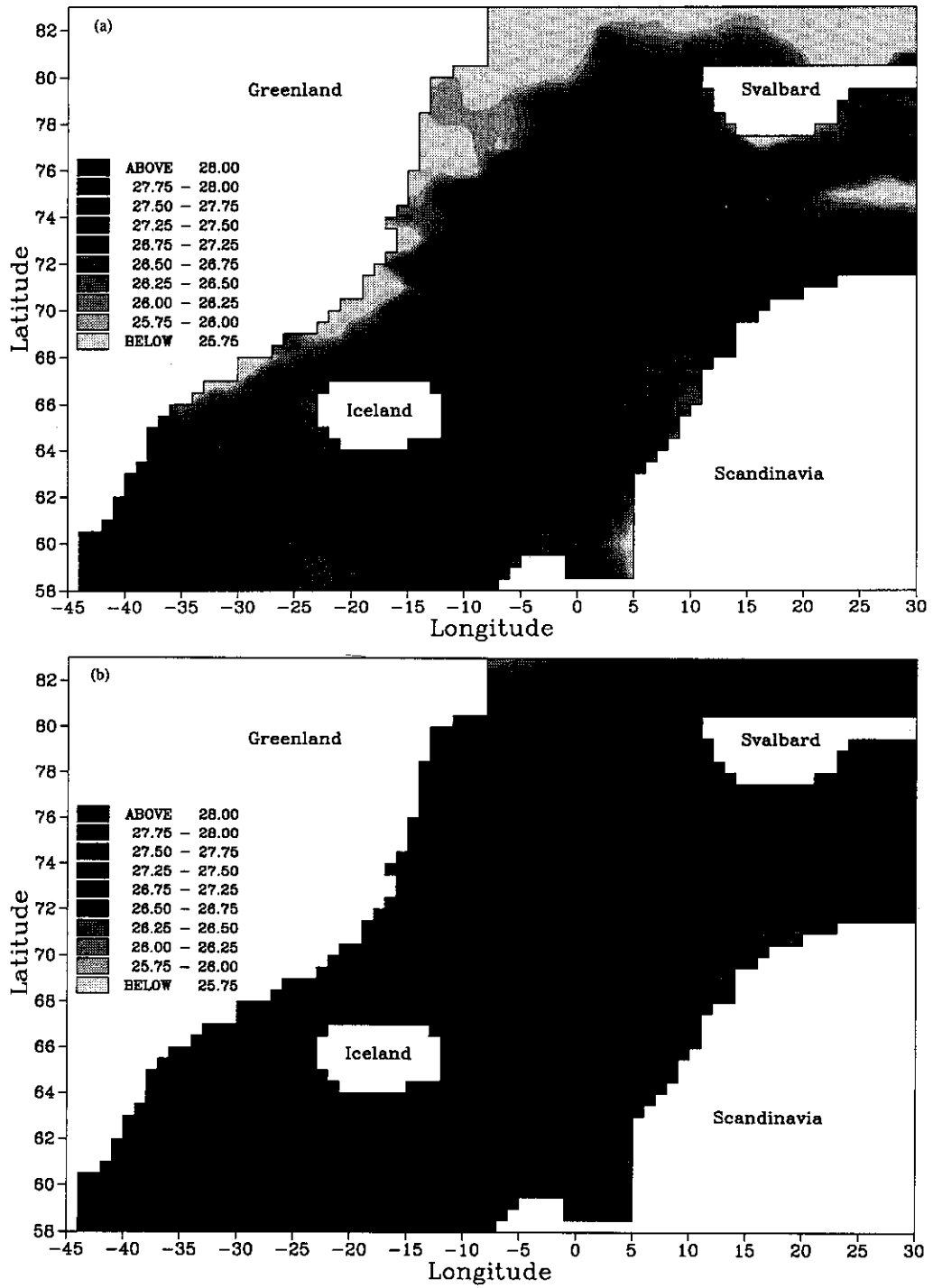


FIG.11. The prescribed surface density for (a) August, September, October and (b) February, March, April. The units are $\text{kg m}^{-3} \cdot 1000$.

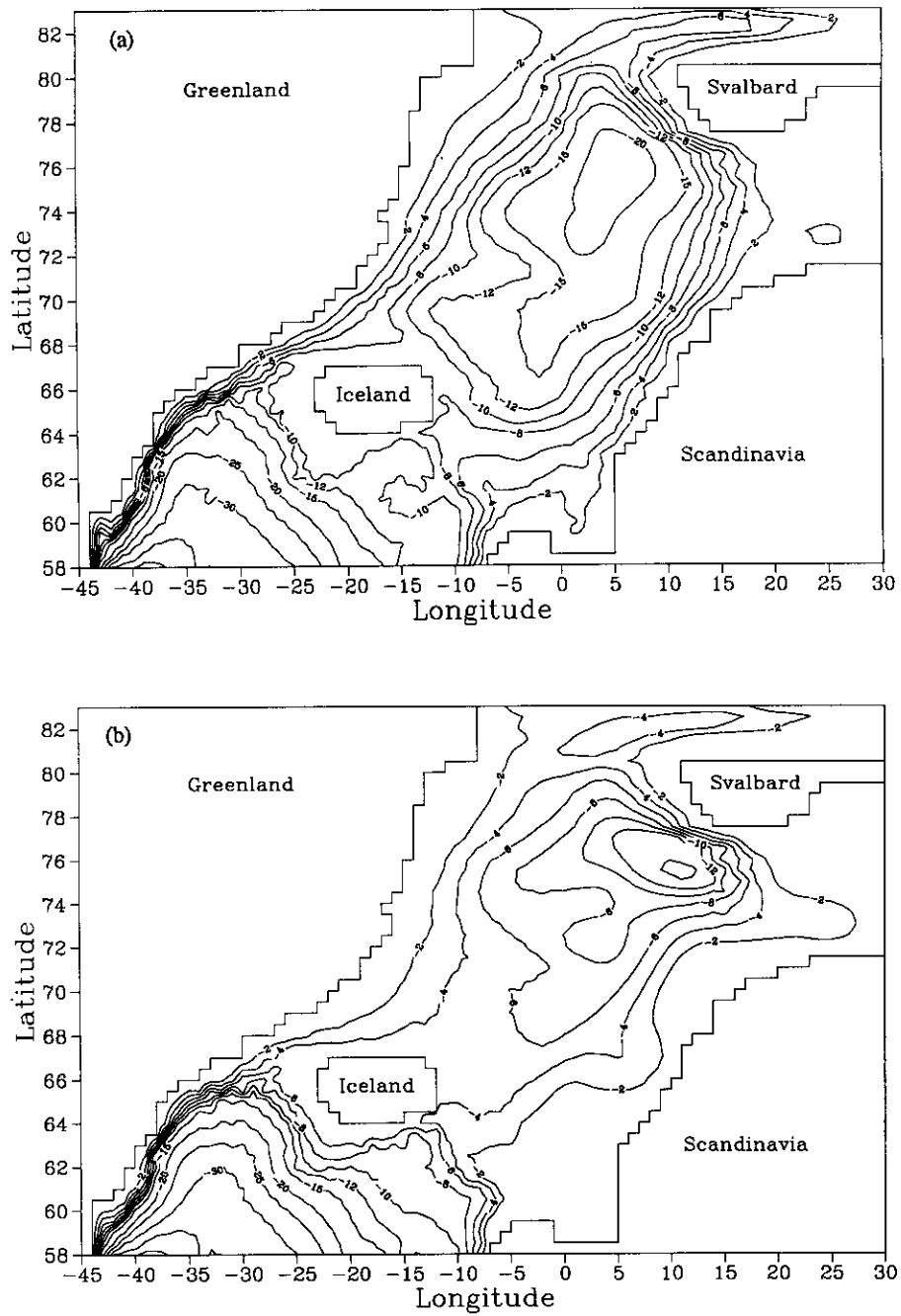


FIG.12. The stream function (in Sverdrups) for (a) November 1982 and (b) May 1983. The contour interval is 2 Sverdrups between -2 and -12 Sverdrups and 5 Sverdrups for values less than -15 Sverdrups.

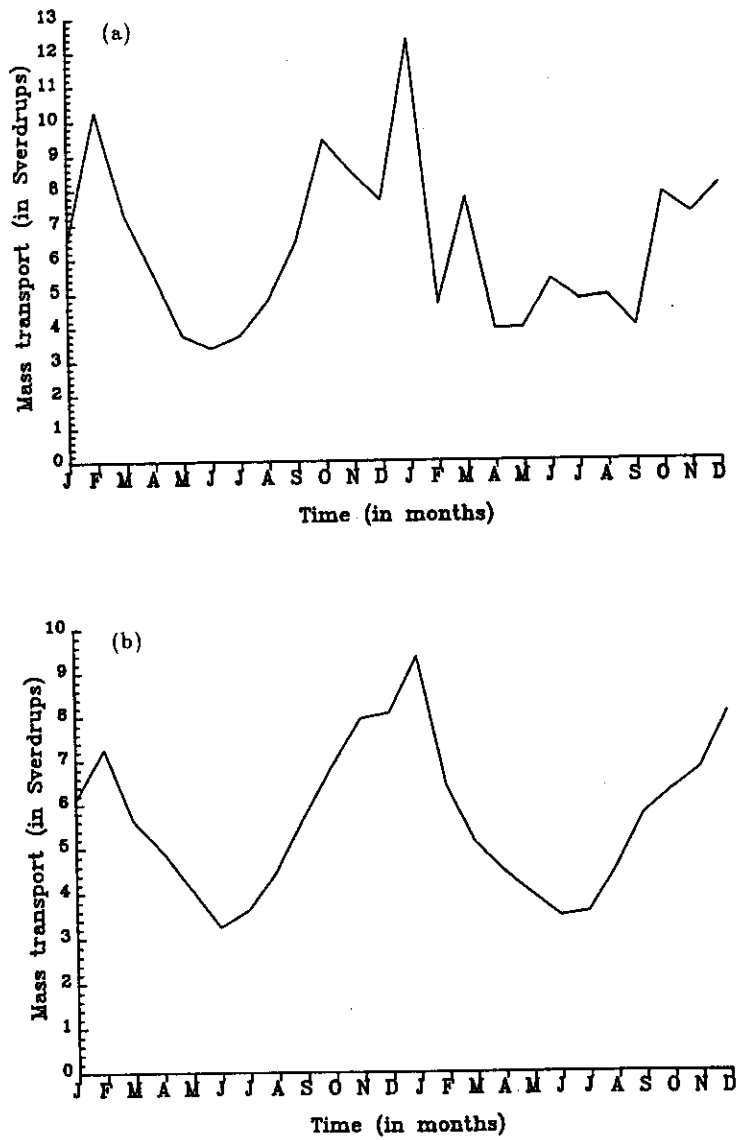


FIG.14. The northward mass transport (in Sverdrups) (a) between Scotland and Iceland and (b) through the Fram Strait, from January 1982 to December 1983.

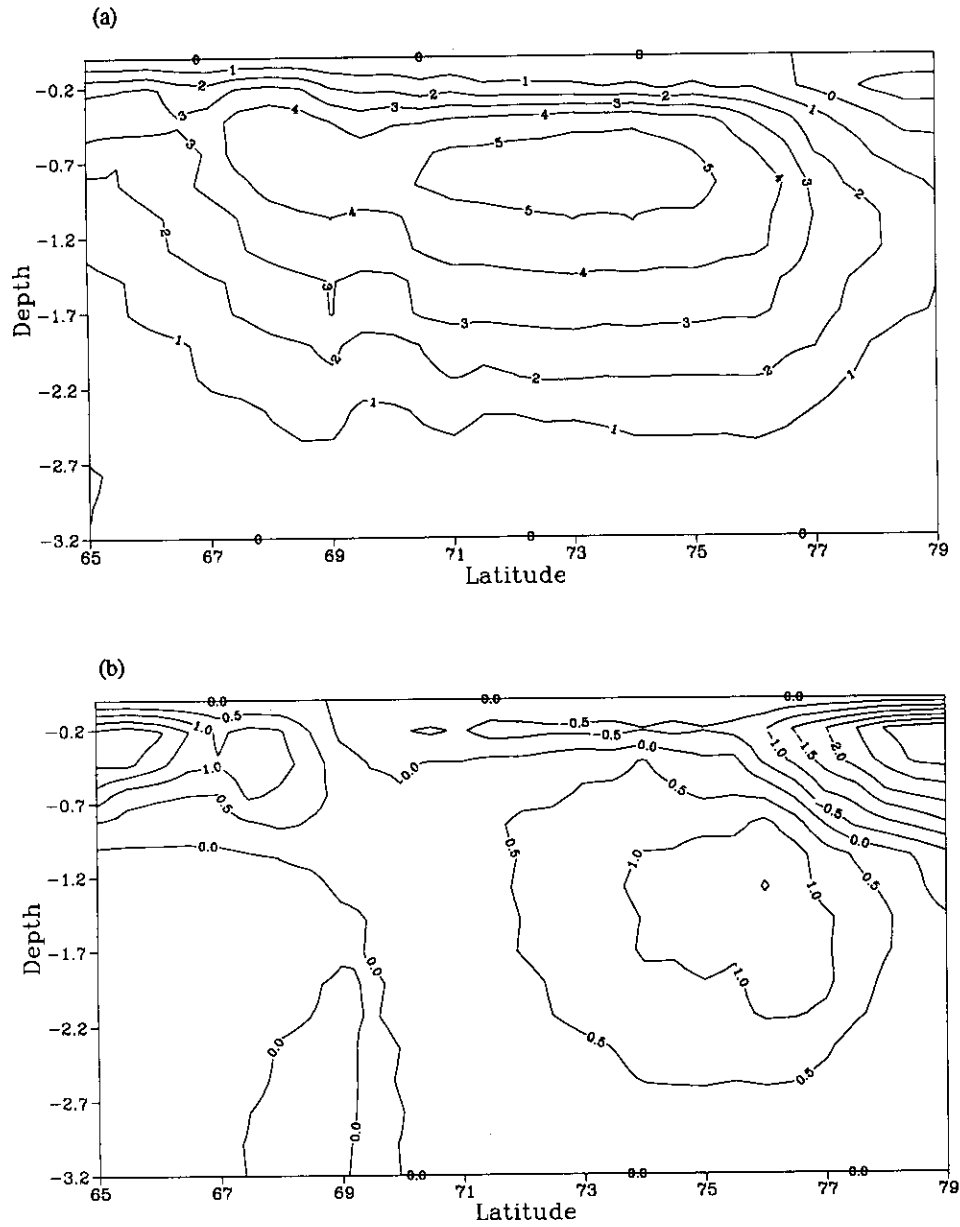


FIG.16. The zonally averaged meridional circulation (in Sverdrups) for (a) February 1982 and (b) September 1983. The depth is in kilometres.

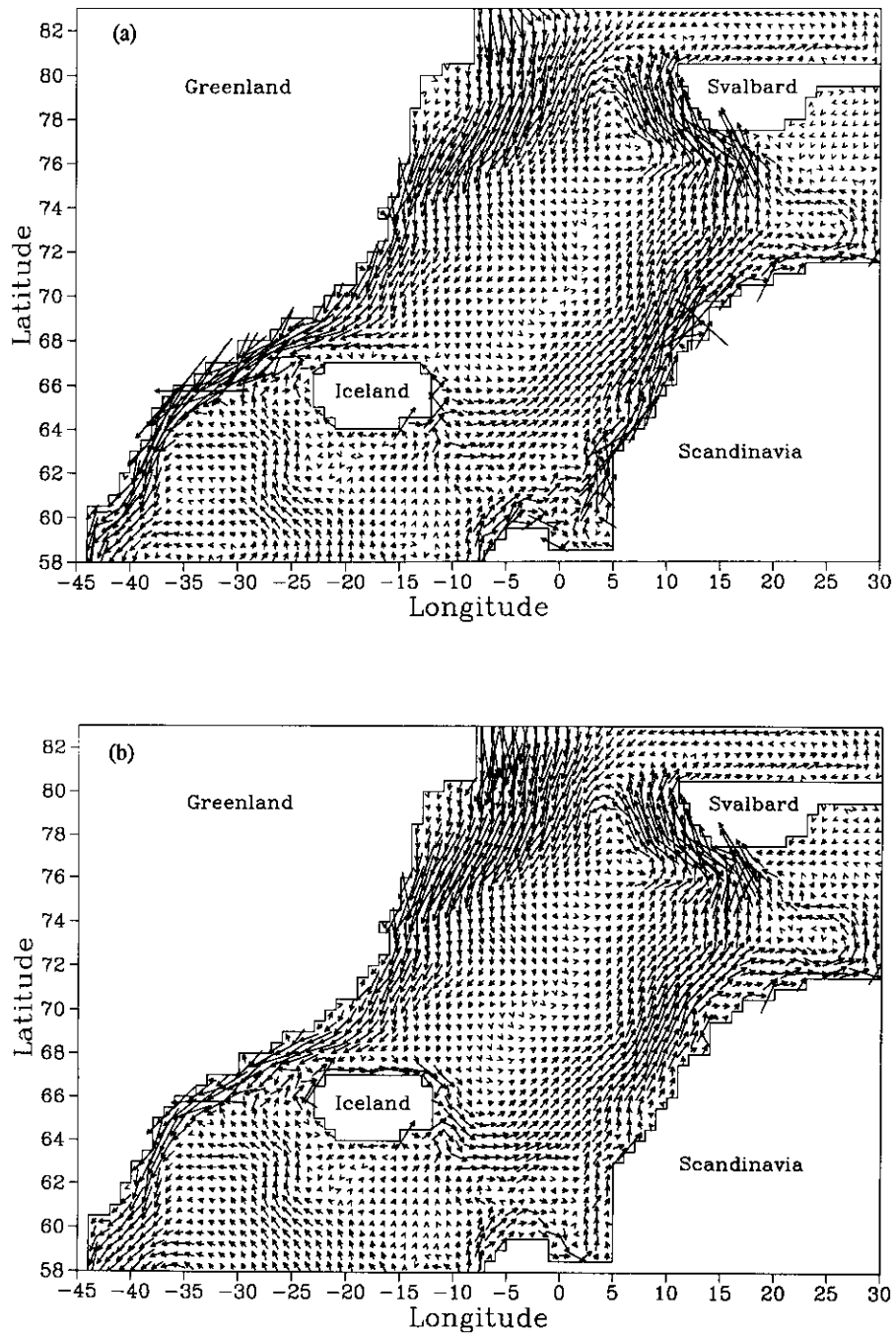


FIG.17. The horizontal velocity at 20m for (a) February 1982 and (b) February 1983. The distance between grid points corresponds to a speed of 5cm s^{-1} .

two branches as it flows southwards from the Arctic Ocean. One branch continues southward along the Greenland shelf while the other follows the Jan-Mayen Ridge. Further south there is another split with the two branches passing either side of Iceland.

We now continue deeper by considering the currents at level 11 (1400m). Figure 20 shows the currents at this level for November 1982 and February 1983. There is a considerable amount of seasonal (and in fact inter-annual) variation at this level, which indicates the important effect of wind forcing. Persistent features include the northward moving deep West Spitsbergen Current and the southward flow on the western side of the Greenland Sea. The southward current in the more central portion of the Greenland Sea is smaller in February 1983 than November 1982 and all but vanishes by May of that year. This is almost certainly a consequence of the wind forcing. As mentioned above, it is trying to induce anticyclonic circulation over the Greenland Sea. This explains why the southward flow has moved toward the eastern side of the Greenland Sea basin. In February 1983 there is a southwards moving undercurrent along the southern edge of the Barents Sea shelf. Further south in the Norwegian Sea the situation is even more variable, southward flow sometimes occurring on the western side of the basin and sometimes on the eastern side. The flow tends to be on the western side from October to April (for the two years modelled) but this is not always the case. Again southward flow dominates.

Turning now to level 14 (2600m) the currents are still variable on both seasonal and inter-annual time scales. Thus it seems that the wind forcing can have an effect on the deepest waters. Figure 21 shows the currents for November 1983. The circulation in the Greenland Sea can only be described as southward. However, at other times the circulation is cyclonic. Currents in the Norwegian Sea tend to be cyclonic in the winter months and southward in the summer months.

An illustration of the surface or near surface temperature, salinity or density fields would be of little value as they are strongly constrained by the surface boundary condition. In fact the basic structure is very much as one would expect given the imposed boundary conditions. It is of greater interest to look at vertical sections of the tracer fields. However for completeness two horizontal sections at deeper levels will be shown. Figure 22(a) illustrates the temperature field at level 8 (520m) for November 1982. The structure is very much as expected given the surface forcing, with the warmest water in the south and east and the coldest water in the north and west. Points of note are the inflow of North Atlantic water which is advected northwards along the Norwegian coast, Barents Sea shelf and past Spitsbergen before entering the Arctic Ocean. This water forms a wedge that is inclined in towards the coast. Warmer water penetrates further north in the summer months. The water over the Greenland Sea basin is always less than 0°C, with the warmer inflow water skirting around the basin. This is in contrast to the run with mean surface forcing where warming occurred, as there was no vertical convection and cooling of the water in this region. Tight fronts exist across the narrow gaps separating the Norwegian Sea from the North Atlantic, the sharpest is at the Iceland-Faroes ridge. Comparing with Fig.3(b) it can be seen that there is no large deviation from the initial temperature field. However the field has become less smooth. Furthermore, the path of the warm North Atlantic water is more consistent with the known currents than the initial field. Figure 22(b) shows the salinity at the same time and depth. The structure of the isohalines are similar to the isothermals in the previous figure. The saline North Atlantic water is advected northwards along the Norwegian coast, while fresher water from the Arctic Ocean is advected southwards along the Greenland side of the sea. Comparing with Fig.3(c) it can be seen that the salinity of the North Atlantic inflow has become more consistent with the current system. Patches of high salinity water are apparent to the West of Spitsbergen. This is caused by the poor quality of the surface boundary data. The surface water in this region is forced cold, saline and thus very dense. This water sinks and spreads out contaminating the deep waters of both the Norwegian and Greenland Seas with water of higher salinity than occurs in reality.

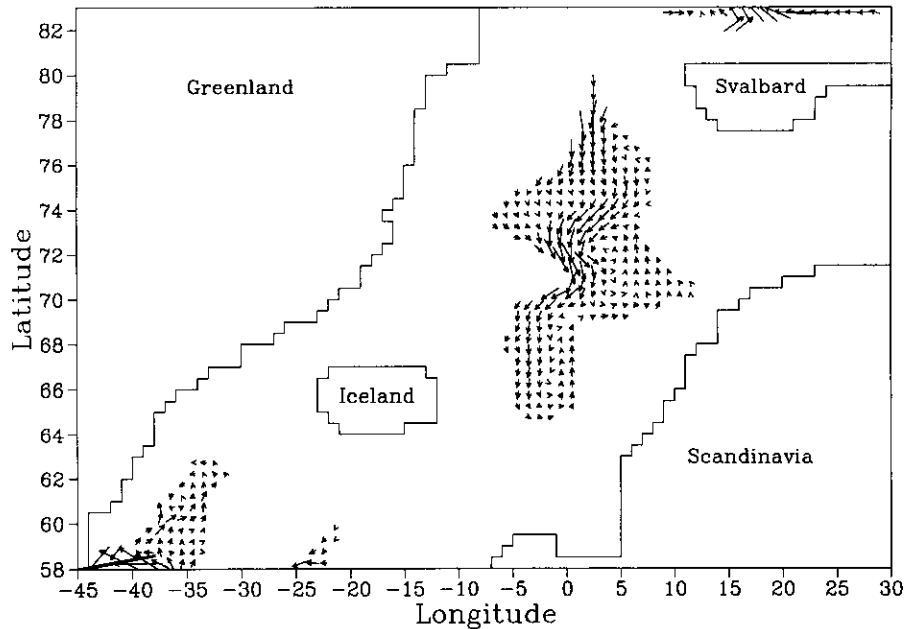


FIG.21. The horizontal velocity at 2600m for November 1983. The distance between grid points corresponds to a speed of 1 cm s^{-1} .

5.4 Vertical sections

Finally attention is turned to vertical sections. Figure 23 shows a north-south section of temperature at 10°E for March 1983. All the expected features occur, including warm surface water in the south and cooler water to the north. The subsurface core of North Atlantic water moving along the Norwegian coast can be clearly seen (as indicated by the 7°C water). In the north the -1°C water indicates a region of convective mixing. The cold surface water mixes down to about 1200m.

East-west temperature and salinity sections at 66°N for August and February 1983 are illustrated in Fig.24. The two pictures give a good indication of the movement of water masses. The temperature section shows northwards moving Atlantic water ($<8^{\circ}\text{C}$), leading onto the continental shelf of Norway to a depth of about 400m. The structure of this wedge is very similar to that observed by HORN and SCHOTT (1976). Further west the water is cooler, with only a shallow warmer layer near the surface. Much of the deep water is nearly isothermal, as is observed by LEE (1963). Immediately to the West of Iceland (in the Denmark Strait), North Atlantic water can be seen moving northwards. Further west is the cold East Greenland Current. Deep in the western corner cold ($<0^{\circ}\text{C}$) water can be seen tilted up against the Greenland coast. This is water of deeper origin that is pushed up over the sill. The tilting up against the coast is caused by the effect of the Earth's rotation (GILL, 1982, p.390). The picture of salinity illustrates several well known features. Moving from west to east, firstly there is the low salinity, East Greenland Current water adjacent to the Greenland coast. To the west of Iceland, northward-moving Atlantic water can be observed, of which the core has sunk beneath lighter fresh water. To the east of Iceland is the relatively fresh, southward-moving East Icelandic Current water. Further east is the main

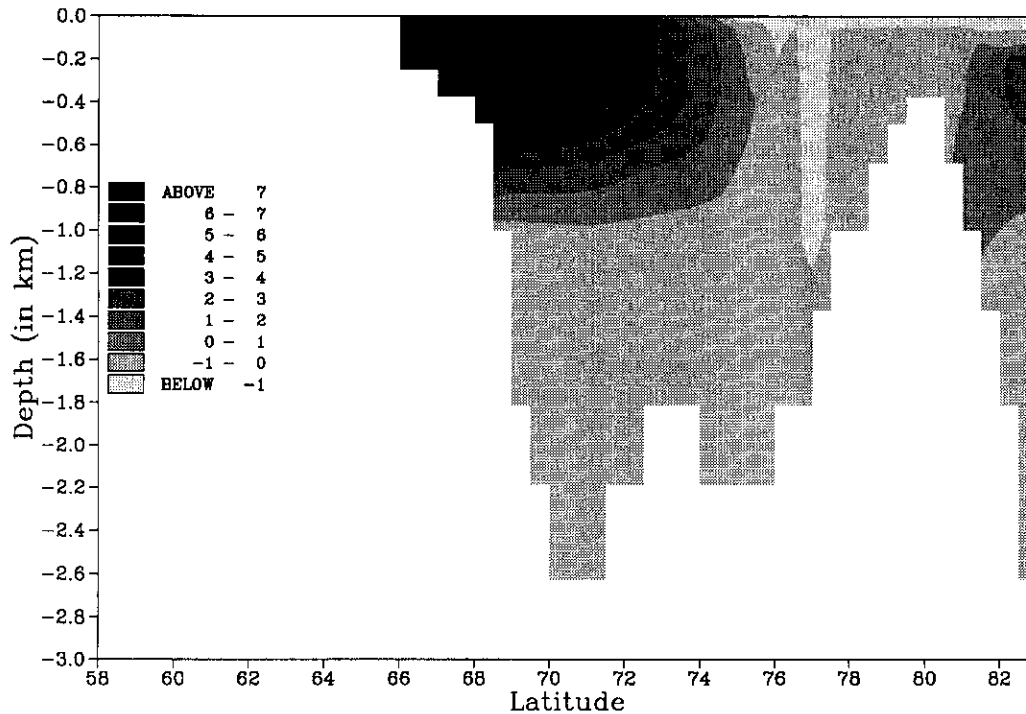


FIG.23. A north-south temperature ($^{\circ}\text{C}$) section at 10°N for March 1983.

bulk of northward-moving North Atlantic water. Again this water leans onto the Norwegian continental slope, where it is overlain by fresh coastal runoff water. The effect of coastal runoff is well reproduced by specifying salinity at the sea surface. The deepest water is of salinity greater than 35 ppt rather than the observed water of about 34.92 ppt, which is caused by the process mentioned at the end of section 5.3. The behaviour of the water masses is very similar to that suggested by HSIEH and GILL (1984). The Atlantic water moves along the eastern coasts and the Norwegian Sea water moves along western coasts. Each water mass travels with the coastline on its right, controlled by the rotation of the Earth.

We now examine a section at 69.5°N , which cuts across the northern part of the Norwegian basin. Figure 25 shows the density field in November 1982. Lighter (fresher) water is apparent at the coasts. In the interior of the basin, the familiar doming up of isopycnals, which enhances the cyclonic circulation, is evident. The northward velocity at this section is illustrated in Fig.26 for May and November 1982. The basic feature of northward flow in the East and southward flow in the West is present in both pictures. However, there is considerable variability. In May there is a stronger northward flow of Atlantic water and a weaker southward flow of polar water than in November. In May the centre of the Atlantic water is pushed off the coast and a southwards flowing undercurrent hugs the Norwegian continental slope, but in November this undercurrent is absent. However, the undercurrent occurs in other months, for instance May 1983 when the picture is almost identical to that in May 1982. This suggests density effects may be dominant here (or that the mean wind was very similar in both years). However an undercurrent is apparent in February 1983, but not in 1982 when there was a particularly large transport northward into the

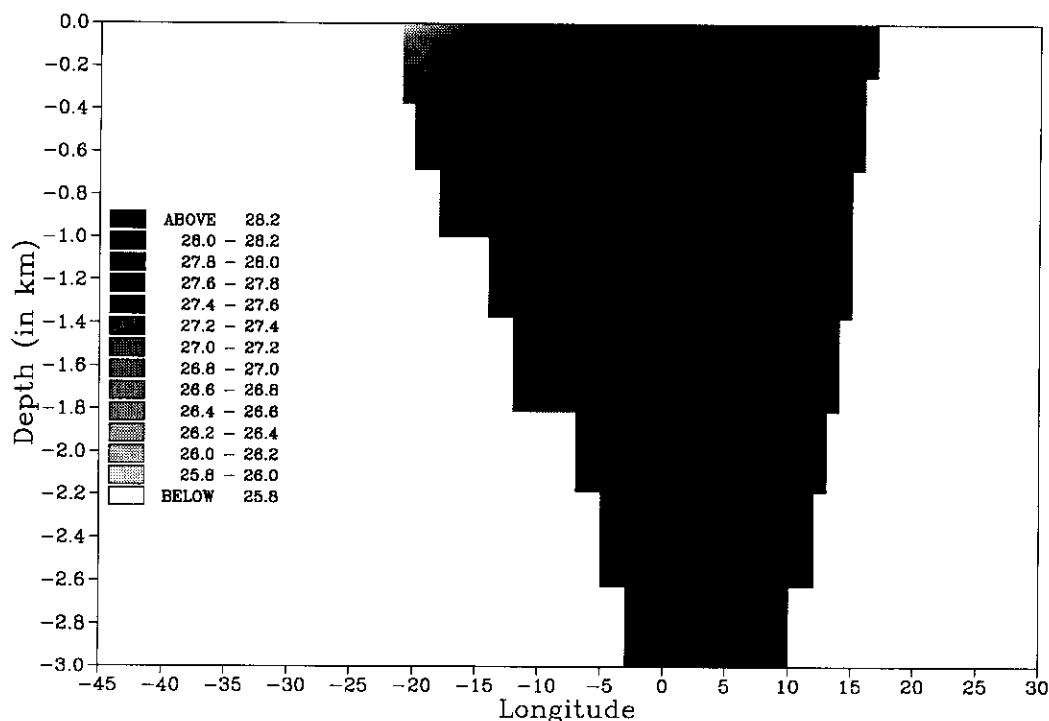


FIG.25. An east-west section at 69.5°N of density σ_ρ ($\text{kg m}^{-3} \cdot 1000$) in November 1982.

Norwegian Sea. Thus the wind driving has an important part to play. In November there is a much smaller northward undercurrent to the East Greenland Current just off the Greenland continental slope. This undercurrent occurs in other months but is always very small.

Finally we look at a section through the Greenland and Barents Seas at 75.5°N . Figure 27 shows the temperature in February 1982. Over the Barents Sea shelf-break the remains of the warm North Atlantic inflow water can be seen as it is advected into the West Spitsbergen Current. In the centre of the basin the isothermals dome upwards, indicating that there is a cyclonic circulation and surface cooling. The cold surface East Greenland Current can be seen adjacent to the Greenland coast, with beneath it a warmer undercurrent which is thought to exist (LEE, 1963). Figure 28 shows the northward velocity at this section for November 1982. The Greenland Sea basin is split into two distinct parts with northwards moving water in the east and southwards moving water in the west. The extremely strong current over the Barents Sea shelf-break is the start of the West Spitsbergen Current. To the west the surface intensified East Greenland Current can be seen against the Greenland coast. The situation here is very similar from month to month, with the main variations being in the strength of the currents.

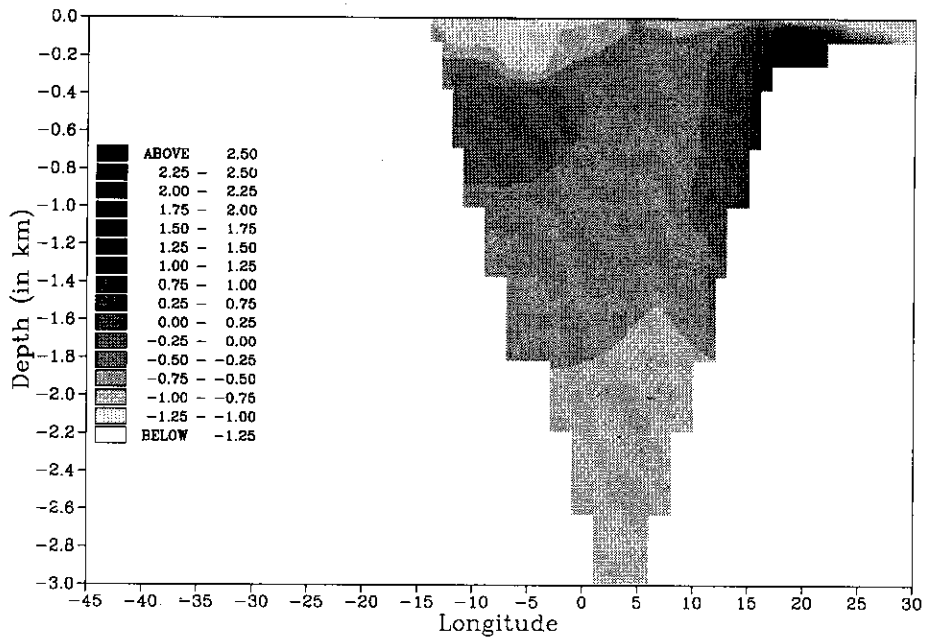


FIG.27. An east-west temperature ($^{\circ}\text{C}$) section at 75.5°N for February 1982.

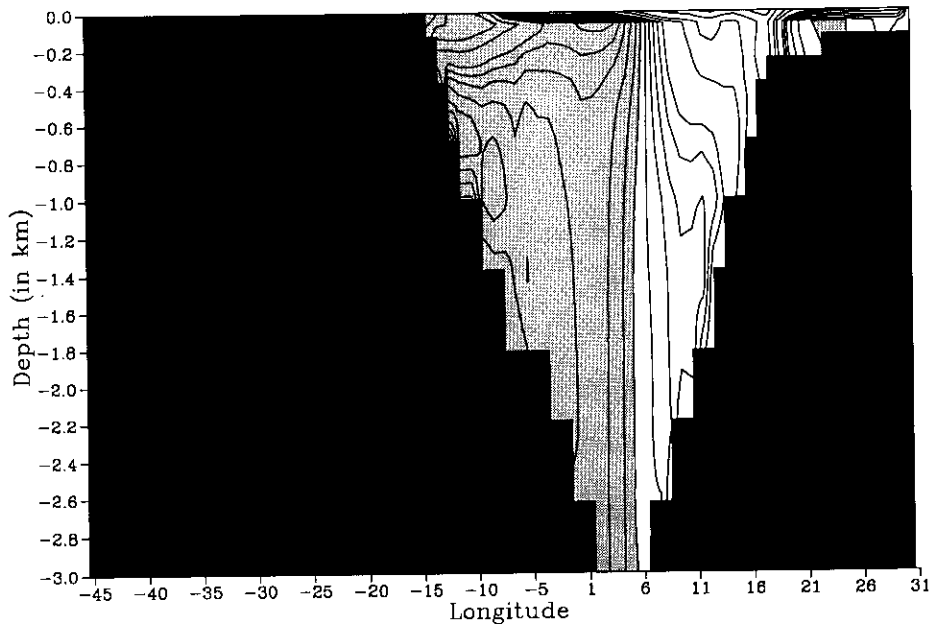


FIG.28. The northward velocity (cm s^{-1}) at 75.5°N for November 1982. Southward flow is shaded. The contour interval is 0, 61, 62, 63, 64, 65, 67.5, 610, 615, 620 cm s^{-1} .

Finally the treatment of vertical mixing in the present generation of three dimensional primitive equation models is in need of substantial improvement. Tests by the author involving a number of different parameterisations for vertical mixing show that the resulting horizontal circulation is sensitive to the method used. Tests by KILLWORTH (1990) have shown how poorly the convection process (which is obviously crucial at high latitude) is represented in these models.

7. ACKNOWLEDGEMENTS

The author wishes to thank Dr John Johnson for much useful discussion during the course of this work. The work was completed in 1988/89 under NERC grant GR3/6716.

8. REFERENCES

- AAGAARD, K. (1970) Wind-driven transports in the Greenland and Norwegian seas. *Deep-Sea Research*, **17**, 281-291.
- AAGAARD, K. and L.K. COACHMAN (1968) The East Greenland Current north of Denmark Strait, Part I. *Arctic*, **21**, 181-200.
- AAGAARD, K. and P. GREISMAN (1975) Toward new mass and heat budgets for the Arctic Ocean. *Journal of Geophysical Research*, **80**, 3821-3827.
- AAGAARD, K., C. DARNALL and P. GREISMAN (1973) Year-long current measurements in the Greenland-Spitsbergen passage. *Deep-Sea Research*, **20**, 743-746.
- ANDERSON, D.L.T. and P.D. KILLWORTH (1977) Spin-up of a stratified ocean, with topography. *Deep-Sea Research*, **24**, 709-732.
- ASSELIN, R. (1972) Frequency filter for time integrations. *Monthly Weather Review*, **100**, 487-490.
- BRYAN, K. (1969) A numerical method for the study of the circulation of the World ocean. *Journal of Computational Physics*, **4**, 347-376.
- BRYAN, K. and M.D. COX (1972) An approximate equation of state for numerical models of Ocean circulation. *Journal of Physical Oceanography*, **2**, 510-514.
- BRYAN, K., S. MANABE and R.C. PACANOWSKI (1975) A global-atmosphere climate model. Part II. The oceanic circulation. *Journal of Physical Oceanography*, **5**, 30-46.
- CARMACK, E. and K. AAGAARD (1973) On the deep water of the Greenland Sea. *Deep-Sea Research*, **20**, 687-715.
- COX, M.D. (1984) *A primitive equation, 3-dimensional model of the ocean*. GFDL Ocean Group Technical Report No.1.
- CREEGAN, A. (1976) A numerical investigation of the circulation in the Norwegian Sea. *Tellus*, **28**, 451-459.
- GILL, A.E. (1982) *Atmosphere-Ocean Dynamics*. Academic Press, London, 662pp.
- HIBLER, W.D. (1979) A dynamic thermodynamic sea ice model. *Journal of Physical Oceanography*, **9**, 815-846.
- HIBLER, W.D. and K. BRYAN (1987) A diagnostic ice-ocean model. *Journal of Physical Oceanography*, **17**, 987-1015.
- HOLLAND, W.R. and A.D. HIRSCHMAN (1972) A numerical calculation of the circulation in the North Atlantic Ocean. *Journal of Physical Oceanography*, **2**, 336-354.
- HOPKINS, T.S. (1988) The Gin Sea, Review of the physical oceanography and literature from 1972. *Saclantcen SR-124*, La Spezia, SACLANT ASW Research Centre.
- HORN, W. and F. SCHOTT (1976) Measurements of stratification and currents at the Norwegian continental slope. *Meteor Forschungsergebnisse, Reihe A*, **18**, 23-63.
- HSEIH, W.W. and A.E. GILL (1984) The Rossby adjustment problem in a rotating, stratified channel, with and without topography. *Journal of Physical Oceanography*, **14**, 424-437.
- KILLWORTH, P.D. (1979) On "chimney" formations in the ocean. *Journal of Physical Oceanography*, **9**, 531-554.
- KILLWORTH, P.D. (1989) On the parameterisation of deep convection in ocean models. In: *'Aha Huliko'a Winter workshop on parameterisation of small-scale processes*, P. MULLER, editor, University of Hawaii, 59-74.